



**HAL**  
open science

## Osmoregulatory performance and immunolocalization of Na<sup>+</sup>/K<sup>+</sup>-ATPase in the branchiopod *Artemia salina* from the Sebkhha of Sidi El Hani (Tunisia)

Imene Sellami, Guy Charmantier, Hachem B. Naceur, Adnane Kacem,  
Catherine Lorin-Nebel

### ► To cite this version:

Imene Sellami, Guy Charmantier, Hachem B. Naceur, Adnane Kacem, Catherine Lorin-Nebel. Osmoregulatory performance and immunolocalization of Na<sup>+</sup>/K<sup>+</sup>-ATPase in the branchiopod *Artemia salina* from the Sebkhha of Sidi El Hani (Tunisia). *Tissue and Cell*, 2020, 63, pp.UNSP 101340. 10.1016/j.tice.2020.101340 . hal-03411067

**HAL Id: hal-03411067**

**<https://hal.umontpellier.fr/hal-03411067>**

Submitted on 7 Mar 2022

**HAL** is a multi-disciplinary open access archive for the deposit and dissemination of scientific research documents, whether they are published or not. The documents may come from teaching and research institutions in France or abroad, or from public or private research centers.

L'archive ouverte pluridisciplinaire **HAL**, est destinée au dépôt et à la diffusion de documents scientifiques de niveau recherche, publiés ou non, émanant des établissements d'enseignement et de recherche français ou étrangers, des laboratoires publics ou privés.



Distributed under a Creative Commons Attribution - NonCommercial | 4.0 International License

1           **Osmoregulatory performance and immunolocalization of Na<sup>+</sup>/K<sup>+</sup>-ATPase in the**  
2           **branchiopod *Artemia salina* from the Sebkhah of Sidi El Hani (Tunisia)**

3  
4  
5  
6 Imene SELLAMI <sup>1,2</sup>, Guy CHARMANTIER <sup>1</sup>, Hachem B. NACEUR <sup>2</sup>, Adnane KACEM <sup>2</sup>,  
7 Catherine LORIN-NEBEL <sup>1\*</sup>

8  
9 <sup>1</sup> Univ. Montpellier, UMR MARBEC (CNRS, IFREMER, IRD, UM), France

10  
11 <sup>2</sup> LR14ES06 Bioressources, Integrative Biology and Valorization, Higher Institute of  
12 Biotechnology of Monastir, University of Monastir, Avenue Tahar Haddad, BP 74, 5000  
13 Monastir, Tunisia

14  
15 \* Corresponding author : Catherine Lorin-Nebel, [catherine.lorin@umontpellier.fr](mailto:catherine.lorin@umontpellier.fr)  
16  
17  
18  
19

20 **Abstract**

21 *Artemia salina* is an extremophile species that tolerates a wide range of salinity, especially  
22 hypertonic media considered lethal for the majority of other aquatic species. In this study, *A.*  
23 *salina* cysts were hatched in the laboratory and nauplii were acclimated at three different  
24 salinities (60, 139 and 212 ppt). Once in the adult phase, their hemolymph osmolality was  
25 measured. The animals were strong hypo-osmoregulators in the entire range of tested  
26 salinities, with up to 10 fold lower hemolymph osmolalities than their surrounding  
27 environment. Immunostaining of Na<sup>+</sup>/K<sup>+</sup>-ATPase was done on sections and on whole body  
28 mounts of adults in order to localize the ionocytes in different organs. An intense Na<sup>+</sup>/K<sup>+</sup>-  
29 ATPase immunostaining throughout the cells was observed in the epithelium of the ten pairs  
30 of metepipodites. A positive immunoreactivity for Na<sup>+</sup>/K<sup>+</sup>-ATPase was also detected in the  
31 maxillary glands, in the epithelium of the efferent tubule and of the excretory canal, as well as  
32 in the anterior digestive tract. This study confirms the strong hypo-osmotic capacity of this  
33 species and affords an overview of the different organs involved in osmoregulation in *A.*  
34 *salina* adults.

35  
36  
37 **Keywords:** *Artemia salina*, hypo-osmoregulation, Na<sup>+</sup>/K<sup>+</sup>-ATPase, immunolocalization,  
38 metepipodites, maxillary glands  
39  
40

## 41 1. Introduction

42

43 *Artemia salina* (Linnaeus, 1758) is part of a complex of euryhaline species of  
44 branchiopod crustaceans qualified as an animal extremophile with an exceptionally wide  
45 salinity tolerance among animals, and particularly an ability to survive and thrive in  
46 hypertonic media, a "forbidden environment" from which most metazoans are excluded as  
47 stated by Eads (2004) (Abatzopoulos et al., 2002; Browne and Bowen, 1991; Clegg and  
48 Trotman, 2002). These animals have attracted the attention of scientists over decades and  
49 have been the subject of extensive studies in order to understand the mechanisms allowing  
50 them to tolerate ionic and osmotic stresses imposed by their environment.

51 These remarkable crustaceans are able to withstand ionic contents and salinities that, in  
52 their upper values, are lethal for the majority of other aquatic species, ranging from 9 ppt  
53 (Brisset et al., 1982) to 340 ppt (Gajardo and Beardmore, 2012; Post and Youssef, 1977) and  
54 up to crystallizing brine close to 600 ppt (Croghan, 1958a, b). *Artemia salina* is a highly  
55 potent hypo-osmotic regulator in media more concentrated than one third of seawater (salinity  
56 of about 11 ppt corresponding to an osmolality of 300 mOsm.kg<sup>-1</sup>). For instance, early studies  
57 had shown that its hemolymph osmolality is maintained between 400 and 800 mOsm.kg<sup>-1</sup> for  
58 salinities ranging from 34 to 340 ppt (1000 to 10 000 mOsm.kg<sup>-1</sup>) (Croghan, 1958b).

59 Such levels of hypo-osmoregulation suppose the existence of powerful ion excretion  
60 abilities in order to compensate the passive invasion of ions from the concentrated external  
61 medium. Moreover, animals have to limit water loss by osmosis, but water uptake  
62 mechanisms are not well known in crustacean, notably in those high-salinity environments. In  
63 larvae, Conte (1984) has extensively described the mechanisms of osmoregulation in the  
64 nauplii of *A. salina* that use a special salt-secreting gland, also called salt gland or neck or  
65 nuchal organ, to excrete salts that penetrate by diffusion. Similarly, Russler and Mangos  
66 (1978) have shown that this organ is the main route for sodium excretion.

67 In adult *A. salina*, different studies have shown a similarity between their mechanisms  
68 of osmoregulation and those proposed for marine teleosts and hypo-regulating crustaceans  
69 (Croghan, 1958b, c, d; Copeland, 1967; Smith, 1969a, b). Brine shrimps have well-developed  
70 active mechanisms for absorbing NaCl from the gut lumen to the hemolymph. Hence, water  
71 follows passively to compensate water lost by osmosis to the external concentrated medium  
72 (Croghan, 1958d). Also in adults, sodium and chloride, which enter the body through  
73 diffusion given their high concentration in the external medium, are excreted to the medium  
74 by specialized organs acting as gills, the metepipodites. The ten pairs of flattened, leaf-like

75 metepipodites borne by the phyllopods have been described as the sites of active outward  
76 transport of ions (Copeland, 1967; Croghan, 1958c).

77 In particular, a detailed study of the metepipodites of *A. salina* was conducted by  
78 Copeland (1967). Using silver nitrate, he confirmed that the metepipodites were the site of ion  
79 (chloride) exchanges, a finding reported earlier by Croghan (1958c) and later confirmed by  
80 other authors (Holliday et al., 1990). Copeland's ultrastructural exploration revealed the  
81 presence and association of two types of cells in the metepipodites, the "light" and "dark  
82 cells". The latter are columnar cells with projected stellate flanges; they extend from the  
83 apical cuticle to the basal membrane lining the hemolymph, i.e. they face the external medium  
84 as well as the hemolymph, and they present deep interdigitations with the light cells. Stacks of  
85 mitochondria, called "mitochondrial pumps" by Copeland, are located in the dark cells in  
86 close association with their membrane, particularly in their projections. From these  
87 observations, Copeland concluded that the metepipodites represent "a highly specialized  
88 tissue for the secretion of salt". Given the location of the dark cells, their ultrastructural  
89 features and particularly the abundance of mitochondria in their cytoplasm, "it would appear  
90 likely that the dark cell is responsible" for the "release of salt to the external environment"  
91 (Copeland, 1967). This hypothesis was confirmed by later experimental findings. In fact, the  
92 crude homogenates of metepipodites showed a very high specific enzyme activity of  $\text{Na}^+/\text{K}^+$ -  
93 ATPase, which increased proportionally with the salinity of the external medium (Holliday et  
94 al., 1990). The same author found that the digestive tract and maxillary glands also had a high  
95  $\text{Na}^+/\text{K}^+$ -ATPase content, which suggests that these organs are also involved in ion transports  
96 and probably for a part in osmoregulatory processes. Membrane-bound  $\text{Na}^+/\text{K}^+$ -ATPase was  
97 partially purified from *A. salina* nauplii (Morohashi and Kawamura, 1984) and the  $\alpha$  isoform  
98 of the enzyme was isolated in salt glands and intestine of nauplii (Cortas et al., 1989). Also in  
99 naupliar larvae,  $\text{Na}^+/\text{K}^+$ -ATPase  $\alpha$  and  $\beta$  isoforms were immunolocalized in the basal  
100 membranes of the salt gland cells (Sun et al., 1991) and the mRNA expression of their  $\alpha 1$  and  
101  $\alpha 2$  isoforms was quantified in the same organs (Conte, 2008; Escalante et al., 1995; Sun et al.,  
102 1992). While the localization of the enzyme is known in the larval salt gland, to our  
103 knowledge surprisingly few reports are available regarding the localization of  $\text{Na}^+/\text{K}^+$ -ATPase  
104 in adult *Artemia*. Recently, an illustration of the presence of  $\text{Na}^+/\text{K}^+$ -ATPase in a  
105 metepipodite of *A. franciscana* has been made available in a preliminary report (Drenth,  
106 2017).

107 The present study aims to confirm the ability of *A. salina* to osmoregulate at very high  
108 salinities, and to determine the localization of Na<sup>+</sup>/K<sup>+</sup>-ATPase in the metepipodites, maxillary  
109 glands and digestive tract of adults, in order to improve the understanding of osmoregulatory  
110 mechanisms allowing a Tunisian *Artemia salina* population (from the hyper-saline lagoon  
111 Sebkhah of Sidi El Hani) to withstand high salinities.

112

## 113 **2. Materials and methods**

114

### 115 *2.1. Cysts sampling*

116

117 *Artemia* cysts were collected in spring 2017 from the banks of the hypersaline Sebkhah  
118 of Sidi El Hani where the salinity exceeded 280 ppt.

119 The Sebkhah of Sidi El Hani is a NW–SE lengthened depression in the Sahel area (eastern  
120 Tunisia) (Fig. 1). The Sidi El Hani discharge area is approximately 370 km<sup>2</sup> and its average  
121 water depth is 0.4 m, and 0.8 m at some locations (Fig. 1). The seasonal temperature  
122 fluctuates between 2 and 13 °C in winter and between 33 and 39 °C in summer (Ali et al.,  
123 2013). The seasonal average of salinity oscillates between a minimum of 180 ppt in winter  
124 registered after rainfall and up to 320 ppt in summer. The ionic composition of Sidi El Hani is  
125 mostly based on Na<sup>+</sup> (115 gL<sup>-1</sup>), Cl<sup>-</sup> (191 gL<sup>-1</sup>), Mg<sup>2+</sup> (8 gL<sup>-1</sup>) and SO<sub>4</sub><sup>2-</sup> (13 gL<sup>-1</sup>). The  
126 presence of *Artemia* in the site was first reported by (Gauthier, 1928).

127

### 128 *2.2. Culture experiments*

129

130 Upon collection, cysts were mixed with salt collected in the Sidi El Hani area, for  
131 conservation. Once in the laboratory, cysts of *Artemia salina* were cleaned, separated and  
132 stored according to the protocol of Sorgeloos *et al.* (1986). Cysts were incubated over 48 hrs  
133 in 1 liter of filtered seawater at a salinity of 35 ppt and a temperature of 25 °C, under constant  
134 illumination (2000 lux) and continuous aeration to keep them in suspension (Lavens and  
135 Sorgeloos, 1996). Following hatching, the nauplii were transferred to 3 containers of 5L filled  
136 with water at different salinities, 60, 139 and 212 ppt. These media had been prepared from a  
137 mixture of seawater sterilized in an autoclave and raw salt (harvested at the Sebkhah of Sidi El  
138 Hani). In each container, the salinity of the water was checked using a salinometer (Lovibond  
139 SensoDirect con110), and the osmolality was measured with an Advanced Instruments 3300  
140 micro-osmometer in later experiments. The containers were placed at a temperature of 25-27

141 °C and a photoperiod of 16 hrs L / 8 hrs D. *Artemia* nauplii density was adjusted to about 50  
142 individuals per L. These larvae were fed twice a week by adding 100 ml of Chlorophyceae  
143 *Dunaliella salina* culture at an approximate density of 100,000 cells.ml<sup>-1</sup> (the salinity of the  
144 microalga culture was the same as that used for the culture of nauplii). Water was renewed  
145 once a week to ensure the elimination of *Artemia salina* waste and agglomerated microalgae.  
146 Once the adult phase was reached, some animals were fixated for histology, others were  
147 transported over 24 hrs in sealed containers to the Marbec laboratory (Montpellier, France)  
148 for further experiments.

149

### 150 2.3. Measure of hemolymph osmolality

151

152 Hemolymph osmolality was measured in 8-12 adult *A. salina* per condition. According  
153 to previous results on different crustacean species (Charmantier, 1998), the animals were  
154 exposed directly to the experimental media for 48 hrs in covered beakers filled with water at  
155 three different salinities maintained at 24 °C, aerated and covered with parafilm to prevent  
156 evaporation. The salinities of the media, 60, 139 and 212 ppt, corresponded to osmolalities of  
157 1737, 4064 and 6192 mOsm.kg<sup>-1</sup>, according to measures made on an Advanced Instrument  
158 Model 3300 micro-osmometer. Prior to sampling, the specimens were carefully rinsed with  
159 deionized water, dried on filter paper and quickly immersed into mineral oil to prevent  
160 evaporation and desiccation. Remaining adherent water was removed using a hand-made  
161 glass micropipette. A second micropipette was then inserted dorsally into the heart to obtain  
162 hemolymph samples, which were then immediately measured with reference to a 300  
163 mOsm.kg<sup>-1</sup> standard solution on a Kalber-Clifton nano-osmometer (Clifton Technical Physics,  
164 Hartford, NY, USA) requiring about 30 nl.

165

### 166 2.4. Histology and immunolocalization of Na<sup>+</sup>/K<sup>+</sup>-ATPase

167

168 In order to localize the ionocytes, and to visualize and semi-quantify Na<sup>+</sup>/K<sup>+</sup>-ATPase,  
169 we performed histology, immunofluorescence staining, whole-mounts and microscopic  
170 observations. About twenty adult brine shrimp from each salinity condition were fixed for 24  
171 hrs by immersion in Bouin's fixative. Once rinsed in several baths of 70 % ethanol, samples  
172 were dehydrated in a graded ethanol series and finally embedded in Paraplast (Sigma).  
173 Longitudinal and transverse sections of 4 µm were cut on a Leitz Wetzlar microtome,  
174 collected on poly-L-lysine coated glass slides and stored at 37 °C for 48 hrs. One series of

175 slides was stained using the Masson's Trichrome staining protocol and observed under a Leica  
176 Diaplan microscope. The other series was used for *in situ* immunolocalization of Na<sup>+</sup>/K<sup>+</sup>-  
177 ATPase. Slides were dewaxed (butanol and LMR), hydrated through a descending series of  
178 ethanol baths (from 100 % to 50 %) and rinsed in phosphate-buffered saline (PBS; 137 mM  
179 NaCl, 2.7 mM KCl, 10 mM phosphate buffer, pH 7.4, Sigma). The slides were then immersed  
180 for 10 min into 0.02 % Tween 20, 150 mM NaCl dissolved in PBS, pH 7.3. After blocking in  
181 5 % skimmed milk (SM) in PBS at 37 °C for 20 min, the slides were rinsed twice with PBS.  
182 Primary labelling was carried out overnight at 4 °C in a wet chamber with the primary  
183 monoclonal antibody ( $\alpha$ 5) mouse anti-Na<sup>+</sup>/K<sup>+</sup>-ATPase (Hybridoma Bank, University of Iowa)  
184 diluted in 0.5% SM-PBS at 10  $\mu$ g.mL<sup>-1</sup>. Using a procedure similar to that of this study, this  
185 antibody was shown to specifically react with Na<sup>+</sup>/K<sup>+</sup>-ATPase in several crustacean species,  
186 such as *Porcellio scaber* (Ziegler, 1997), *Homarus gammarus* (Lignot et al., 1999), *Astacus*  
187 *leptodactylus* (Lignot et al., 2004), *Carcinus maenas* (Cieluch et al., 2004), *Crangon crangon*  
188 (Cieluch et al., 2005), *Eriocheir sinensis* (Cieluch et al., 2007), *Macrobrachium amazonicum*  
189 (Boudour-Bouchecker et al., 2014) and *Eurytemora affinis* (Gerber et al., 2016). Once rinsed  
190 three times in PBS to remove unbound primary antibody, the sections were incubated for 1 hr  
191 with a secondary antibody (donkey anti-mouse Alexa Fluor® 488 (Invitrogen, Life  
192 Technologies) at 10  $\mu$ g.mL<sup>-1</sup> in SM-PBS) and rinsed again three times in PBS. Nuclei of  
193 some slides were counterstained using DAPI at 1 $\mu$ g/ml for 6 min, followed by three washes in  
194 PBS.

195 Several protocols of preparation and immunostaining of whole mounts of *A. salina*  
196 have been tried. A limitation of antibody penetration was encountered probably due to the  
197 cuticle barrier. EDTA, ultrasonic treatment from 5 s to 2 min, and Triton X-100 were tested in  
198 different combinations. Positive staining was obtained using ultrasonic pulses at 35 KHz from  
199 10 s to 20 s as indicated thereafter. Even in the best preparations, only some metepipodites of  
200 the animals showed positive staining. Following pretreatment with ultrasonic pulses (from 10  
201 s to 20 s) to enhance probe accessibility, whole mounts of *A. salina* adults were pre-incubated  
202 in 5 % skimmed milk (SM) in PBS and 0.3 % Triton X-100 (PBS-TX) for 2 hrs at room  
203 temperature. After blocking, the animals were rinsed several times with PBS. Primary  
204 labelling was carried out overnight at 4 °C in a wet chamber with the primary monoclonal  
205 antibody ( $\alpha$ 5) mouse anti-Na<sup>+</sup>/K<sup>+</sup>-ATPase (Hybridoma Bank, University of Iowa) diluted at  
206 10  $\mu$ g.mL<sup>-1</sup> in 0.5 % SM-PBS. Following three rinses in PBS, the specimens were incubated  
207 for 3 hrs with a secondary antibody (donkey anti-mouse Alexa Fluor® 488 (Invitrogen, Life

208 Technologies) at  $10 \mu\text{g.mL}^{-1}$ ) and rinsed again in PBS. Nuclei of some mounts were  
209 counterstained using DAPI at  $1 \mu\text{g.mL}^{-1}$  for 6 min, followed by three washes in PBS.

210 Sections and whole mount preparations were then mounted in an anti-bleaching  
211 mounting medium (Immunohistomount, Santa Cruz Biotechnology) and observed with a  
212 Leica Diaplan microscope equipped with a special filter for fluorescence (450-490 nm) and  
213 coupled to a Leica DC300F digital camera and FW4000 software. Observations and  
214 photography of selected slides were conducted using a Leica TCS SP2 confocal microscope  
215 of the MRI platform, Montpellier University.

216

### 217 *2.5. Quantification of the $\text{Na}^+/\text{K}^+$ -ATPase (NKA) immunostaining intensity in* 218 *phyllopods*

219

220 To determine the relative importance of different phyllopods in ion transport in each  
221 salinity condition, we compared the relative fluorescence intensity of immunostaining in  
222 metepipodites of *Artemia* adults. Several photographs were taken in 5 individuals for each  
223 studied salinity using a constant exposure time. Longitudinal sections were used to visualize  
224 the different metepipodites and their  $\text{Na}^+/\text{K}^+$ -ATPase content within an animal.

225 The photographs were analyzed using the public domain ImageJ software (version 1.49, v),  
226 according to a protocol successfully used in other crustaceans (Boudour-Bouchecker et al.,  
227 2013; Gerber et al., 2016; Issartel et al., 2010) and in fish (Ouattara et al., 2009; Riou et al.,  
228 2012; Sucré et al., 2012). The intensity of immunostaining, i.e. the staining intensity of the  
229 immunolabelled area, was measured by quantifying the pixel intensity of the immunolabeled  
230 area using ImageJ software. These measurements were performed using the ImageJ software's  
231 "Average Gray Value" parameter, which determines the sum of the gray values of all pixels in  
232 the selected area relative to the number of pixels, expressed in calibrated units (optical  
233 density). In a second step, the ImageJ software was used to quantify the difference in average  
234 pixel intensity of fluorescence between different salinities among metepipodites within the  
235 same adults.

236

### 237 *2.6. Statistics*

238 Statistical analyses (hemolymph osmolality and fluorescence intensity) were performed  
239 using Graphpad Prism (version 6, GraphPad Software Incorporated, La Jolla, CA 268, USA).  
240 Normality and homogeneity of variance were respectively checked using D'Agostino-Pearson  
241 test and Barlett's test. For data fitting homogeneity of variance requirement, a one-way



242 ANOVA regarding or regardless salinity as the main factor was performed; critical  
243 differences between groups were appraised using the Tukey's multiple comparisons test. For  
244 data not fitting homogeneity of variance and data due to the small sample size, a non-  
245 parametric Kruskal-Wallis test followed by a multiple comparisons Dunn's test was used.  
246 Data are presented as means  $\pm$  SD, and the level of statistical significance was set at  $p < 0.05$ .

247

248

### 249 **3. Results**

250

251 The main results of this study are summarized in Fig. 1S.

252

#### 253 *3.1. Hemolymph osmolality*

254

255 *Artemia* adults were extremely strong hypo-osmoregulators. Their hemolymph  
256 osmolality, which ranged between  $406 \pm 21$  and  $608 \pm 16$  mOsm.Kg<sup>-1</sup> in our experiment, was  
257 significantly different according to salinity (Fig. 2; one-way ANOVA,  $p < 0.001$ ). It is worth  
258 noting that hemolymph osmolalities differed by only 202 mOsm.Kg<sup>-1</sup> between the lower and  
259 higher tested salinities that themselves differed by more than 4450 mOsm.Kg<sup>-1</sup>.

260

#### 261 *3.2. Morphological description*

262

263 The morphology of *Artemia* adults is illustrated in Fig. 3. Eleven pairs of phyllopod  
264 (Ph1-11) were observed. The ten pairs of flattened leaf-like metepipodites are attached at the  
265 middle part of the ten phyllopods, (Me1-10). The eleventh pair of phyllopods is sexually  
266 dimorphic between the sexes and does not bear a metepipodite (Fig. 3A, 4A, B, C, 5A, B).  
267 Each metepipodite is a flattened leaf-like oval structure (Fig. 3A, C, 5G), with average  
268 minimum and maximum dimensions of  $225 \pm 50$   $\mu$ m and  $486 \pm 84$   $\mu$ m. Metepipodites 1 and 2  
269 are smaller (Fig. 3A).

270 Internally, we observed a longitudinal digestive tract, and a pair of maxillary glands  
271 located on each side of the digestive tract in the anterior part of the body (Fig. 6).

272

#### 273 *3.3. Histology and immunolocalization of Na<sup>+</sup>/K<sup>+</sup>-ATPase (NKA)*

274

275 Metepipodites are flat structures formed of two identical facing monolayered epithelia  
276 covered by a thin cuticle, limiting a hemolymph lacuna (Fig. 5). A hemolymphatic space at  
277 the base of each metepipodite allows a communication with the phyllopod (Fig. 5C, D). NKA  
278 localization was visualized using immunohistochemical analysis of longitudinal and  
279 transverse sections. An intense immunostaining throughout most of the cells was observed in  
280 the epithelium of the ten pairs of metepipodites (Figs 3B, C, 4C, 5). The immunopositive cells  
281 were large ( $57\pm 3\ \mu\text{m}$  cellules) and contained a voluminous nucleus with average diameter of  
282  $10\pm 1\ \mu\text{m}$  (Fig. 5F, F'). Immunostaining intensity appears lower in some cells (Figs 3C, 5G).

283

284 The semi-quantification of fluorescence intensity of metepipodites showed no  
285 significant difference between the different metepipodites and among the analyzed salinities  
286 and an overall high variability was observed between animals (Fig. 2S).

287

288 A positive immunoreactivity for  $\text{Na}^+/\text{K}^+$ -ATPase was detected in the maxillary glands,  
289 where a strong immunostaining was observed in the epithelium of the efferent tubule and in  
290 the excretory canal (Fig. 6C-H). The proximal coelomic sac was not immunostained (Fig.  
291 6C). The anterior digestive tract revealed a positive immunolabelling in the basal cell part as  
292 shown in Fig. 6D-F.

293 Negative control sections without the primary antibody did not show immunolabelling  
294 in any organ or tissue (not shown).

295

296

#### 297 **4. Discussion**

298

299 Brine shrimps, *Artemia* species, are usually considered as extremophiles especially for  
300 their ability to face challenging salinities (up to 10-fold that of standard seawater) considered  
301 lethal for the majority of other aquatic species (Gajardo and Beardmore, 2012). Such  
302 environmental pressures demand an ability to regulate hemolymph osmolytes according to the  
303 external medium via powerful osmoregulatory mechanisms (Campbell et al., 2012;  
304 Charmantier et al., 2009; Freire et al., 2003). Blood osmolality change is often used as an  
305 indicator for osmoregulatory acclimation and tolerance to salinity stress (Varsamos et al.,  
306 2005). This study has confirmed the hypo-osmotic capacity of *Artemia* adults that can  
307 maintain their hemolymph osmolality up to 10 fold lower than their surrounding environment  
308 (for example hemolymph osmolality of  $608 \pm 16\ \text{mOsm.Kg}^{-1}$  in a medium at  $6192\ \text{mOsm.Kg}^{-1}$

309 <sup>1</sup>, 212 ppt). Due to these exceptional physiological abilities, brine shrimps are considered the  
310 most powerful hypo-osmoregulators among aquatic metazoans, with the highest tolerance to  
311 salinity (Cole and Brown, 1967). Extensive similar studies have concluded that the  
312 hemolymph osmotic pressure was markedly hypotonic even in the most concentrated media  
313 (Medwedewa, 1927; Plattner, 1955). Holliday *et al.* (1990) stated that *A. salina* is a weak  
314 hyporegulator in 50 % SW and an increasingly strong hyporegulator in 100 %, 200 % and 400  
315 % SW. Different studies have also shown a similarity between the mechanisms of  
316 osmoregulation in *Artemia* adults and those proposed for marine teleosts and hypo-regulating  
317 crustaceans (Croghan, 1958b, c, d; Copeland, 1967; Thuet *et al.*, 1968; Smith, 1969a, b).  
318 Croghan (1958b, c, d), in an extensive study of osmoregulation in brine shrimps, has shown  
319 that they have well-developed active mechanisms for absorbing NaCl from the gut lumen to  
320 the hemolymph, resulting in a passive influx of water to hemolymph that compensates water  
321 lost by osmosis to the external concentrated medium (Croghan, 1958d). Sodium and chloride,  
322 which also enter the body through diffusion given their high concentration in the external  
323 medium, are excreted to the medium by specialized organs.

324  
325 Na<sup>+</sup>/K<sup>+</sup>-ATPase is known as the major driving force that ensures ion exchanges (Cieluch *et*  
326 *al.*, 2004; Geering, 2008; Lignot *et al.*, 1999; Lignot and Charmantier, 2001; Lucu and Towle,  
327 2003; Thabet *et al.*, 2016; Thuet *et al.*, 1988) as well as generating an electrical gradient  
328 fuelling other transporters (Campbell *et al.*, 2012; Esbaugh *et al.*, 2019; Pivovarov *et al.*,  
329 2019; Sáez *et al.*, 2009). Its abundance in an organ suggests an involvement in ion transport.  
330 The present study affords an overview of the different organs involved in osmoregulation in  
331 *A. salina* adults. Immunofluorescence staining of Na<sup>+</sup>/K<sup>+</sup>-ATPase was used in order to  
332 localize ionocytes in these organs.

333 Previous studies first addressed osmoregulation in embryos and during early post-  
334 embryonic development. Several extensive studies have reported that active ion excretion  
335 mediated by Na<sup>+</sup>/K<sup>+</sup>-ATPase is carried out by the naupliar salt gland (or dorsal / neck / nuchal  
336 organ) that develops in late pre-naupliar embryonic stages; this organ becomes apparently  
337 functional shortly before hatching. Later in development, thoracic epipodites take over ion  
338 transport according to the stage of development (Conte, 1984; Conte *et al.*, 1977, 1972;  
339 Mitchell and Crews, 2002; Peterson *et al.*, 1978; Russler and Mangos, 1978; Thuet, 1982).  
340 Working in naupliar larvae, Sun *et al.* (1991) reported that Na<sup>+</sup>/K<sup>+</sup>-ATPase  $\alpha$  and  $\beta$  subunits  
341 were immunolocalized in the basal membranes of the salt gland cells. The mRNA expression

342 of  $\alpha 1$  and  $\alpha 2$  paralogs was quantified in the same organs (Conte, 2008; Escalante et al., 1995;  
343 Sun et al., 1991).

344 In the present study, an intense  $\text{Na}^+/\text{K}^+$ -ATPase immunostaining throughout most of the  
345 cells was observed in the epithelium of the ten pairs of metepipodites. Our results confirm  
346 those found in earlier works that attributed active outward transport of ions to metepipodites  
347 in adults (Copeland, 1967; Croghan, 1958c; Holliday et al., 1990). In a major study using  
348 electron microscopy, Copeland (1967) concluded that the metepipodites represent “a highly  
349 specialized tissue for the secretion of salt and a special cell type found in these structures (the  
350 'dark cell'), rich in mitochondria, is thought to be responsible for this ion transport”. The  
351 numerous immunostained cells that we observed in metepipodites therefore correspond to the  
352 “dark cells” as described by Copeland (1967). As we detected no difference in  
353 immunostaining intensity among metepipodites, this suggests a similar cellular  $\text{Na}^+/\text{K}^+$ -  
354 ATPase content among different metepipodites and an involvement of all metepipodites in  
355 active transport. Later experimental findings conducted on crude homogenates of  
356 metepipodites revealed a very high specific enzyme activity of  $\text{Na}^+/\text{K}^+$ -ATPase, which  
357 increased proportionally with the salinity of the external medium (Holliday et al., 1990). A  
358 slight but not significant increase in immunostaining intensity has been observed between 60  
359 and 139 ppt and could indicate a slightly increased  $\text{Na}^+/\text{K}^+$ -ATPase content within the cells  
360 lining phyllopods at 139 ppt. Recently, a preliminary report of Drenth (2017) confirmed the  
361 presence of  $\text{Na}^+/\text{K}^+$ -ATPase in a metepipodite of *A. franciscana* and the salt extrusion occurs  
362 in a mitochondrial rich, membraneous cell layer in the metepipodites of the brine shrimp. The  
363 same investigator suggested that brine shrimp upregulate only the  $\alpha 2$  form of  $\text{Na}^+/\text{K}^+$ -ATPase  
364 in response to increasing salinity, while the  $\alpha 1$  form remains relatively unchanged.

365 A positive immunoreactivity for  $\text{Na}^+/\text{K}^+$ -ATPase was also detected in the anterior digestive  
366 tract and in the maxillary glands. In these paired glands,  $\text{Na}^+/\text{K}^+$ -ATPase immunostaining was  
367 observed in the epithelium of the efferent tubule and of the excretory canal, while the  
368 coelomic sac remained unstained. Our results confirmed that these organs are also involved in  
369 ion transport and probably for a part in osmoregulatory processes. In the same context, Tyson  
370 (1969) had shown that the efferent duct of the maxillary gland of *A. salina* presents  
371 ultrastructural features typical of transporting epithelia. Holliday *et al.* (1990) measured a  
372 high  $\text{Na}^+/\text{K}^+$ -ATPase activity in the digestive tract. Studying the physiology of the gut in *A.*  
373 *salina* and its implication in osmoregulation, Croghan (1958c) found that the concentration of  
374 both sodium and chloride ions in the gut fluids was always lower than that in the hemolymph,  
375 pointing to an active uptake of NaCl across the gut epithelium, which in turn controls water

376 balance and prevents dehydration in hypertonic media. Indeed, Drenth (2017) confirmed the  
 377 basolateral localization of Na<sup>+</sup>/K<sup>+</sup>-ATPase in the gut of *A. franciscana* adults, where ions and  
 378 water are taken in from the environment into the hemolymph (Russler and Mangos, 1978).

379

## 380 **5. Conclusion**

381

382 In this work, we have focused on the hypo-osmoregulatory capacity of adult *A. salina*  
 383 and particularly on their main organs involved in active ion transport. We have confirmed that  
 384 brine shrimps are powerful hypo-osmoregulators as they keep their hemolymph osmolality  
 385 strongly lower than even the most concentrated media. Immunofluorescence and whole  
 386 mounts staining of Na<sup>+</sup>/K<sup>+</sup>-ATPase have been used to illustrate the histological and cellular  
 387 structure of metepipodites related to osmoregulation; despite their major function, their  
 388 functional histology had surprisingly not been re-addressed since the major works of the  
 389 1960's. We have also confirmed the involvement in osmoregulation of the maxillary glands  
 390 and of the anterior part of the digestive tract.

391

392

## 393 **Acknowledgements**

394 The authors would like to thank Sophie Hermet for her assistance in histology and the  
 395 Montpellier Ressources Imaging (MRI-DBS UM) platform and notably Elodie Jublanc for her  
 396 help in confocal microscopy.

397

## 398 **List of References**

399

- 400 Abatzopoulos, T.J., Kappas, I., Bossier, P., Sorgeloos, P., Beardmore, J.A., 2002. Genetic  
 401 characterization of *Artemia tibetiana* (Crustacea: Anostraca). *Biol. J. Linn. Soc.* 75, 333–344.  
 402 <https://doi.org/10.1046/j.1095-8312.2002.00023.x>
- 403 Boudour-Bouchecker, N., Boulo, V., Charmantier-Daures, M., Grousset, E., Anger, K., Charmantier,  
 404 G., Lorin-Nebel, C., 2014. Differential distribution of V-type H<sup>+</sup>-ATPase and Na<sup>+</sup>/K<sup>+</sup>-ATPase in  
 405 the branchial chamber of the palaemonid shrimp *Macrobrachium amazonicum*. *Cell Tissue Res.*  
 406 357, 195–206. <https://doi.org/10.1007/s00441-014-1845-5>
- 407 Boudour-Bouchecker, N., Boulo, V., Lorin-Nebel, C., Elguero, C., Grousset, E., Anger, K.,  
 408 Charmantier-Daures, M., Charmantier, G., 2013. Adaptation to freshwater in the palaemonid  
 409 shrimp *Macrobrachium amazonicum*: comparative ontogeny of osmoregulatory organs. *Cell*  
 410 *Tissue Res.* 353, 87–98. <https://doi.org/10.1007/s00441-013-1622-x>
- 411 Brisset, P., Versichele, D., Bossuyt, E., De Ruyck, L., Sorgeloos, P., 1982. High density flow-through

- 412 culturing of brine shrimp *Artemia* on inert feeds-preliminary results with a modified culture  
413 system. *Aquac. Eng.* 1, 115–119. [https://doi.org/10.1016/0144-8609\(82\)90003-6](https://doi.org/10.1016/0144-8609(82)90003-6)
- 414 Browne, R.A., Bowen, S.T., 1991. Taxonomy and population genetics of *Artemia*, in: Browne, R.A.,  
415 Sorgeloos, P., Trotman, C.N.A. (Eds.), *Artemia Biology*. CRC Press, Boca Raton, Florida,  
416 U.S.A, pp. 221–235.
- 417 Campbell, J., Samuel, M., Faria, C., 2012. Evolution of osmoregulatory patterns and gill ion transport  
418 mechanisms in the decapod Crustacea : a review. *J Comp Physiol B* 182, 997–1014.  
419 <https://doi.org/10.1007/s00360-012-0665-8>
- 420 Charmantier, G., 1998. Ontogeny of osmoregulation in crustaceans: a review. *Invertebr. Reprod. Dev.*  
421 33, 177–190. <https://doi.org/10.1080/07924259.1998.9652630>
- 422 Charmantier, G., Charmantier-Daures, M., Towle, D., 2009. Osmotic and ionic regulation in aquatic  
423 arthropods, in: Evans, D.H. (Ed.), *Osmotic and Ionic Regulation: Cells and Animals*. CRC Press,  
424 New York, pp. 165–208.
- 425 Cieluch, U., Anger, K., Aujoulat, F., Buchholz, F., Charmantier-Daures, M., Charmantier, G., 2004.  
426 Ontogeny of osmoregulatory structures and functions in the green crab *Carcinus maenas*  
427 (Crustacea, Decapoda). *J. Exp. Biol.* 207, 325–336. <https://doi.org/10.1242/jeb.00759>
- 428 Cieluch, U., Anger, K., Charmantier-Daures, M., Charmantier, G., 2007. Osmoregulation and  
429 immunolocalization of Na<sup>+</sup>/K<sup>+</sup>-ATPase during the ontogeny of the mitten crab *Eriocheir sinensis*  
430 (Decapoda, Grapsoidea). *Mar. Ecol. Prog. Ser.* 329, 169–178.  
431 <https://doi.org/10.3354/meps329169>
- 432 Cieluch, U., Charmantier, G., Grousset, E., Charmantier-Daures, M., Anger, K., 2005.  
433 Osmoregulation, immunolocalization of Na<sup>+</sup>/K<sup>+</sup>-ATPase, and ultrastructure of branchial epithelia  
434 in the developing brown shrimp, *Crangon crangon* (Decapoda, Caridea). *Physiol. Biochem.*  
435 *Zool.* 78, 1017–1025. <https://doi.org/10.1086/432856>
- 436 Clegg, J., Trotman, C.N.A., 2002. Physiological and biochemical aspects of *Artemia* ecology. *Artemia*  
437 *Basic Appl. Biol.* 1, 129–170. [https://doi.org/10.1007/978-94-017-0791-6\\_3](https://doi.org/10.1007/978-94-017-0791-6_3)
- 438 Cole, G.A., Brown, R.J., 1967. The chemistry of *Artemia* habitats. *Ecology* 48, 858–861.  
439 <https://doi.org/10.2307/1933745>
- 440 Conte, F.P., 2008. Molecular domains in epithelial salt cell NaCl of crustacean salt gland (*Artemia*).  
441 *Int. Rev. Cell Mol. Biol.* 268, 39–57. [https://doi.org/10.1016/S1937-6448\(08\)00802-2](https://doi.org/10.1016/S1937-6448(08)00802-2)
- 442 Conte, F.P., 1984. Structure and function of the crustacean larval salt gland, in: Bourne, G.H.,  
443 Danielli, J.F., Jeon, K.W. (Eds.), *International Review of Cytology*. Academic Press, pp. 45–106.  
444 [https://doi.org/10.1016/S0074-7696\(08\)61314-5](https://doi.org/10.1016/S0074-7696(08)61314-5)
- 445 Conte, F.P., Droukas, P.C., Ewing, R.D., 1977. Development of sodium regulation and de novo  
446 synthesis of Na<sup>+</sup>, K<sup>+</sup>-activated ATPase in larval brine shrimp, *Artemia salina*. *J. Exp. Zool.* 202,  
447 339–361. <https://doi.org/10.1002/jez.1402020306>
- 448 Conte, F.P., Hootman, S.R., Harris, P.J., 1972. Neck organ of *Artemia salina* nauplii. *J. Comp.*

- 449       Physiol. 80, 239–246. <https://doi.org/10.1007/bf00694838>
- 450 Copeland, D.E., 1967. A study of salt secreting cells in the brine shrimp (*Artemia salina*). *Protoplasma*
- 451       63, 363–384.
- 452 Cortas, N., Arnaut, M., Salon, J., Edelman, I.S., 1989. Isoforms of Na, K-ATPase in *Artemia salina*:
- 453       II. Tissue distribution and kinetic characterization. *J. Membr. Biol.* 108, 187–195.
- 454       <https://doi.org/10.1007/bf01871029>
- 455 Croghan, P.C., 1958a. The survival of *Artemia salina* (L.) in various media. *J. Exp. Biol.* 35, 213–218.
- 456 Croghan, P.C., 1958b. The osmotic and ionic regulation of *Artemia salina* (L.). *J. Exp. Biol.* 35, 219–
- 457       233.
- 458 Croghan, P.C., 1958c. The mechanism of osmotic regulation in *Artemia salina* (L.): the physiology of
- 459       the branchiae. *J. Exp. Biol.* 35, 234–242.
- 460 Croghan, P.C., 1958d. The mechanism of osmotic regulation in *Artemia salina* (L.): The physiology of
- 461       the gut. *J. Exp. Biol.* 35, 243–249.
- 462 Drenth, J., 2017. Altered Na, K-ATPase isoform expression in *Artemia franciscana* in response to
- 463       hypersaline environments. Thesis Diss. <https://doi.org/10.30707/ETD2017.Drenth.J>
- 464 Eads, B.D., 2004. Salty survivors: *Artemia*: basic and applied biology. *J. Exp. Biol.* 207, 1757–1758.
- 465       <https://doi.org/10.1242/jeb.01005>
- 466 Esbaugh, A.J., Brix, K. V, Grosell, M., 2019. Na<sup>+</sup>, K<sup>+</sup>-ATPase isoform switching in zebrafish during
- 467       transition to dilute freshwater habitats. *Proc. R. Soc. B* 286.
- 468       <https://doi.org/10.1098/rspb.2019.0630>
- 469 Escalante, R., García-Sáez, A., Sastre, L., 1995. In situ hybridization analyses of Na, K-ATPase alpha-
- 470       subunit expression during early larval development of *Artemia franciscana*. *J. Histochem.*
- 471       *Cytochem.* 43, 391–399. <https://doi.org/10.1177/43.4.7897181>
- 472 Freire, C.A., Cavassin, F., Rodrigues, E.N., Torres, A.H., McNamara, J.C., 2003. Adaptive patterns of
- 473       osmotic and ionic regulation, and the invasion of fresh water by the palaemonid shrimps. *Comp.*
- 474       *Biochem. Physiol. Part A Mol. Integr. Physiol.* 136, 771–778.
- 475       <https://doi.org/10.1016/j.cbpb.2003.08.007>
- 476 Gajardo, G.M., Beardmore, J.A., 2012. The brine shrimp *Artemia*: adapted to critical life conditions.
- 477       *Front. Physiol.* 3, 1–8. <https://doi.org/10.3389/fphys.2012.00185>
- 478 Gauthier, H., 1928. Recherches sur la faune des eaux continentales de l'Algérie et de la Tunisie.
- 479       Thesis Diss. Minerva, Alger, Algeria.
- 480 Geering, K., 2008. Functional roles of Na,K-ATPase subunits. *Curr. Opin. Nephrol. Hypertens.* 17,
- 481       526–532. <https://doi.org/10.1097/MNH.0b013e3283036cbf>
- 482 Gerber, L., Lee, C.E., Grousset, E., Blondeau-Bidet, E., Boucheker, N.B., Lorin-Nebel, C.,
- 483       Charmantier-Daures, M., Charmantier, G., 2016. The legs have it: In situ expression of ion
- 484       transporters V-type H<sup>+</sup>-ATPase and Na<sup>+</sup>/K<sup>+</sup>-ATPase in the osmoregulatory leg organs of the
- 485       invading copepod *Eurytemora affinis*. *Physiol. Biochem. Zool.* 89, 233–250.

- 486 <https://doi.org/10.1086/686323>
- 487 Holliday, C.W., Roye, D.B., Roer, R.D., 1990. Salinity-induced changes in branchial Na<sup>+</sup>/K<sup>+</sup>-ATPase  
488 activity and transepithelial potential difference in the brine shrimp *Artemia salina*. J. Exp. Biol.  
489 151, 279–296.
- 490 Issartel, J., Boulo, V., Wallon, S., Geffard, O., Charmantier, G., 2010. Cellular and molecular  
491 osmoregulatory responses to cadmium exposure in *Gammarus fossarum* (Crustacea,  
492 Amphipoda). Chemosphere 81, 701–710. <https://doi.org/10.1016/j.chemosphere.2010.07.063>
- 493 Lavens, P., Sorgeloos, P., 1996. Manual on the production and use of live food for aquaculture., FAO  
494 Tech. Pap. Food and Agriculture Organization (FAO), Rome, Italy.
- 495 Lignot, J.-H., Charmantier-Daures, M., Charmantier, G., 1999. Immunolocalization of Na<sup>+</sup>/K<sup>+</sup>-ATPase  
496 in the organs of the branchial cavity of the european lobster *Homarus gammarus* (Crustacea,  
497 Decapoda). Cell Tissue Res. 296, 417–426. <https://doi.org/10.1007/s004410051301>
- 498 Lignot, J.-H., Charmantier, G., 2001. Immunolocalization of Na<sup>+</sup>, K<sup>+</sup>-ATPase in the branchial cavity  
499 during the early development of the european lobster *Homarus gammarus* (Crustacea,  
500 Decapoda). J. Histochem. Cytochem. 49, 1013–1023.  
501 <https://doi.org/10.1177/002215540104900809>
- 502 Lignot, J.-H., Susanto, G.N., Charmantier-Daures, M., Charmantier, G., 2004. Immunolocalization of  
503 Na<sup>+</sup>, K<sup>+</sup>-ATPase in the branchial cavity during the early development of the crayfish *Astacus*  
504 *leptodactylus* (Crustacea, Decapoda). Cell Tissue Res. 319, 331–339.  
505 <https://doi.org/10.1007/s00441-004-1015-2>
- 506 Lucu, Č., Towle, D.W., 2003. Na<sup>+</sup>, K<sup>+</sup>-ATPase in gills of aquatic crustacea. Comp. Biochem. Physiol.  
507 Part A Mol. Integr. Physiol. 135, 195–214. [https://doi.org/10.1016/S1095-6433\(03\)00064-3](https://doi.org/10.1016/S1095-6433(03)00064-3)
- 508 Medwedewa, N.B., 1927. Über den osmotischen Druck der Hämolymphe von *Artemia salina*. J.  
509 Comp. Physiol. A Neuroethol. Sensory, Neural, Behav. Physiol. 5, 547–554.
- 510 Mitchell, B., Crews, S.T., 2002. Expression of the *Artemia* tracheless gene in the salt gland and  
511 epipod. Evol. Dev. 4, 344–353. <https://doi.org/10.1046/j.1525-142X.2002.02023.x>
- 512 Morohashi, M., Kawamura, M., 1984. Solubilization and purification of *Artemia salina* (Na, K)-  
513 activated ATPase and NH<sub>2</sub>-terminal amino acid sequence of its larger subunit. J. Biol. Chem.  
514 259, 14928–14934.
- 515 Ouattara, N., Bodinier, C., Nègre-Sadargues, G., D’Cotta, H., Messad, S., Charmantier, G., Panfili, J.,  
516 Baroiller, J.-F., 2009. Changes in gill ionocyte morphology and function following transfer from  
517 fresh to hypersaline waters in the tilapia *Sarotherodon melanotheron*. Aquaculture 290, 155–164.  
518 <https://doi.org/10.1016/j.aquaculture.2009.01.025>
- 519 Peterson, G.L., Ewing, R.D., Conte, F.P., 1978. Membrane differentiation and de novo synthesis of the  
520 (Na<sup>+</sup>/ K<sup>+</sup>)-activated adenosine triphosphatase during development of *Artemia salina* nauplii. Dev.  
521 Biol. 67, 90–98. [https://doi.org/10.1016/0012-1606\(78\)90302-0](https://doi.org/10.1016/0012-1606(78)90302-0)
- 522 Pivovarov, A.S., Calahorro, F., Walker, R.J., 2019. Na<sup>+</sup> / K<sup>+</sup> - pump and neurotransmitter membrane



- 523 receptors. *Invertebr. Neurosci.* 19, 1–16. <https://doi.org/10.1007/s10158-018-0221-7>
- 524 Plattner, F., 1955. Der osmotische Druck von *Artemia salina*. *Pflüger's Arch. für die gesamte Physiol.*  
 525 des Menschen und der Tiere 261, 172–182. <https://doi.org/10.1007/bf00369788>
- 526 Post, F.J., Youssef, N.N., 1977. A procaryotic intracellular symbiont of the Great Salt Lake brine  
 527 shrimp *Artemia salina* (L.). *Can. J. Microbiol.* 23, 1232–1236. <https://doi.org/10.1139/m77-184>
- 528 Riou, V., Ndiaye, A., Budzinski, H., Dugué, R., Le Ménach, K., Combes, Y., Bossus, M., Durand, J.-  
 529 D., Charmantier, G., Lorin-Nebel, C., 2012. Impact of environmental DDT concentrations on gill  
 530 adaptation to increased salinity in the tilapia *Sarotherodon melanotheron*. *Comp. Biochem.*  
 531 *Physiol. Part C Toxicol. Pharmacol.* 156, 7–16. <https://doi.org/10.1016/j.cbpc.2012.03.002>
- 532 Russler, D., Mangos, J., 1978. Micropuncture studies of the osmoregulation in the nauplius of *Artemia*  
 533 *salina*. *Am. J. Physiol. Integr. Comp. Physiol.* 234, R216–R222.  
 534 <https://doi.org/10.1152/ajpregu.1978.234.5.R216>
- 535 Sáez, A.G., Lozano, E., Zaldívar-Riverón, A., 2009. Evolutionary history of Na, K-ATPases and their  
 536 osmoregulatory role. *Genetica* 136, 479–490. <https://doi.org/10.1007/s10709-009-9356-0>
- 537 Smith, P.G., 1969a. The ionic relations of *Artemia salina* (L.): I. Measurements of electrical potential  
 538 difference and resistance. *J. Exp. Biol.* 51, 727–738.
- 539 Smith, P.G., 1969b. The ionic relations of *Artemia salina* (L.): II. Fluxes of sodium, chloride and  
 540 water. *J. Exp. Biol.* 51, 739–757.
- 541 Sorgeloos, P., Lavens, P., Léger, P., Tackaert, W., Versichele, D., 1986. Manual for the culture and  
 542 use of brine shrimp *Artemia* in aquaculture. *Artemia Ref. Center, Faculty of Agriculture, State*  
 543 *Univ. Ghent, Belgium.*
- 544 Sucré, E., Vidussi, F., Mostajir, B., Charmantier, G., Lorin-Nebel, C., 2012. Impact of ultraviolet-B  
 545 radiation on planktonic fish larvae: Alteration of the osmoregulatory function. *Aquat. Toxicol.*  
 546 109, 194–201. <https://doi.org/10.1016/j.aquatox.2011.09.020>
- 547 Sun, D.Y., Guo, J.Z., Hartmann, H.A., Uno, H., Hokin, L.E., 1992. Differential expression of the  
 548 alpha 2 and beta messenger RNAs of Na, K-ATPase in developing brine shrimp as measured by  
 549 in situ hybridization. *J. Histochem. Cytochem.* 40, 555–562.  
 550 <https://doi.org/10.1177/40.4.1313064>
- 551 Sun, D.Y., Guo, J.Z., Hartmann, H.A., Uno, H., Hokin, L.E., 1991. Na, K-ATPase expression in the  
 552 developing brine shrimp *Artemia*. *Immunochemical localization of the alpha-and beta-subunits.*  
 553 *J. Histochem. Cytochem.* 39, 1455–1460. <https://doi.org/10.1177/39.11.1655875>
- 554 Tagorti, M.A., Essefi, E., Touir, J., Guellala, R., Yaich, C., 2013. Geochemical controls of  
 555 groundwaters upwelling in saline environments : Case study the discharge playa of Sidi El Hani  
 556 (Sahel, Tunisia). *J. African Earth Sci.* 86, 1–9. <https://doi.org/10.1016/j.jafrearsci.2013.05.004>
- 557 Thabet, R., Rouault, J., Ayadi, H., Leignel, V., 2016. Structural analysis of the  $\alpha$  subunit of  $\text{Na}^+/\text{K}^+$   
 558 ATPase genes in invertebrates. *Comp. Biochem. Physiol. Part B Biochem. Mol. Biol.* 196, 11–  
 559 18. <https://doi.org/10.1016/j.cbpb.2016.01.007>

- 560 Thuet, P., 1982. Adaptations écophysiologicals d'*Artemia* (Crustacé, Branchiopode, Anostracé) aux  
561 variations de salinité. Bull. la société d'écophysologie 7, 203–225.
- 562 Thuet, P., Charmantier-Daures, M., Charmantier, G., 1988. Relation entre osmorégulation et activités  
563 d'ATPase Na<sup>+</sup>-K<sup>+</sup> et d'anhydrase carbonique chez larves et postlarves de *Homarus gammarus*  
564 (L.)(Crustacea: Decapoda). J. Exp. Mar. Bio. Ecol. 115, 249–261.
- 565 Thuet, P., Motais, R., Maetz, J., 1968. Les mécanismes de l'euryhalinité chez le crustacé des salines  
566 *Artemia salina* L. Comp. Biochem. Physiol. 26, 793–818.
- 567 Tyson, G.E., 1969. Intercoil connections of the kidney of the brine shrimp, *Artemia salina*. Z.  
568 Zellforsch. 100, 54–59.
- 569 Varsamos, S., Nebel, C., Charmantier, G., 2005. Ontogeny of osmoregulation in postembryonic fish: a  
570 review. Comp. Biochem. Physiol. Part A Mol. Integr. Physiol. 141, 401–429.
- 571 Ziegler, A., 1997. Immunocytochemical localization of Na<sup>+</sup>, K<sup>+</sup>-ATPase in the calcium-transporting  
572 sternal epithelium of the terrestrial isopod *Porcellio scaber* L. (Crustacea). J. Histochem. Cytochem.  
573 45, 437–446. <https://doi.org/10.1177/002215549704500311>

574

575

576 **Legends of Figures**

577

578 Abbreviations. ADT: anterior digestive tract; Cs: coelomic sac; E: eye; EC: excretory canal; Me:  
579 metepipodite; MG: maxillary gland; N: nucleus; Ph: phyllopod; PI: posterior intestine; T: tubule.

580

581 **Fig. 1.** Geographical location of the Sebkhha of Sidi El Hani (Tunisia). Google Earth Pro V. 7.3.2.5776.

582

583 **Fig. 2.** Adult *Artemia salina*. Osmotic pressure of the hemolymph of animals maintained at three  
584 different salinities (60 ppt: 1737 mOsm.Kg<sup>-1</sup>, 139 ppt: 4064 mOsm.Kg<sup>-1</sup>, 212 ppt: 6192 mOsm.Kg<sup>-1</sup>,  
585 N=8-12). The dotted line is the isosmotic line. Different letters indicate significant differences  
586 (p<0.001).

587

588 **Fig. 3.** Adult *Artemia salina*. Morphology and localization of metepipodites (Me) and maxillary  
589 glands (MG). (A) Dorsal view showing the eleven pairs of phyllopods (Ph) and the ten pairs of  
590 metepipodites. (B), (C) Whole-mounts and immunolocalization of Na<sup>+</sup>/K<sup>+</sup>-ATPase; (B) Anterior view  
591 with immunostaining in the two maxillary glands and in one metepipodite 1; (C) Median view with  
592 several phyllopods and immunostained metepipodites. Scale bars: (A) 500 µm; (B), (C) 200 µm.

593

594 **Fig. 4.** Adult *Artemia salina*. Localization of metepipodites (Me) on phyllopods (Ph). (A), (B)  
595 Longitudinal vertical and horizontal histological sections. (C) Longitudinal horizontal section:

596 immunolocalization of Na<sup>+</sup>/K<sup>+</sup>-ATPase in metepipodites 1-9 attached to phyllopods. Scale bars: (A),  
597 (B) 500 μm, (C) 40 μm.

598

599 **Fig. 5.** Adult *Artemia salina*. Histological structure and immunolocalization of Na<sup>+</sup>/K<sup>+</sup>-ATPase (NKA)  
600 and DNA staining of nuclei on phyllopods and metepipodites sections. (A), (B), (F), (F') Merged  
601 staining of Na<sup>+</sup>/K<sup>+</sup>-ATPase (green) and DNA (blue). (C), (D), (E) Phyllopods bearing metepipodites  
602 with NKA immunostaining (D, E) or Trichrome Masson's staining (C). (G) Immunolocalization of  
603 NKA on metepipodites in horizontal (Me4) and transverse (Me5, 6) sections. Scale bars: (A), (B) 40  
604 μm; (C), (D), (E), (F), (G) 20 μm; (F') 5 μm.

605

606 **Fig. 6.** Adult *Artemia salina*. Histological structure, whole-mounts and immunolocalization of Na<sup>+</sup>/K<sup>+</sup>-  
607 ATPase (NKA) in the anterior digestive tract (ADT), in the maxillary gland (MG), and in  
608 metepipodite (Me). (A), (B) Transverse histological sections of the anterior digestive tract and of the  
609 maxillary gland. (C), (D), (E) NKA localization in transverse sections of the anterior digestive tract  
610 and of the maxillary gland. (F) Horizontal section of the anterior digestive tract and of the two  
611 maxillary glands. (G), (H) Whole mounts showing NKA localization in the maxillary gland and  
612 metepipodite 1. Scale bars: (A), (B), (C), (D), (F) 20 μm; (E) 40 μm; (G) 200 μm; (H) 50 μm.

613

614 **Fig. 1S.** Present results (in red) and previous knowledge on osmoregulation in the branchiopod  
615 *Artemia* at different development stages involving different osmoregulatory organs.

616

617 **Fig. 2S.** Adult *Artemia salina*. Relative immunostaining intensity for Na<sup>+</sup> /K<sup>+</sup>-ATPase (NKA) in the  
618 different metepipodites (1-10) and its difference according to different salinities. (A) Comparison  
619 between the metepipodites (1-10) regardless of salinity (N=5-6). (B) Comparison between the studied  
620 salinities regardless of the location of metepipodite (N=3-12).

621

622

623

624

625

626

627



Fig. 1.

628  
629  
630  
631  
632  
633  
634  
635  
636  
637  
638  
639  
640  
641  
642  
643  
644  
645  
646  
647  
648  
649  
650  
651  
652  
653  
654  
655  
656

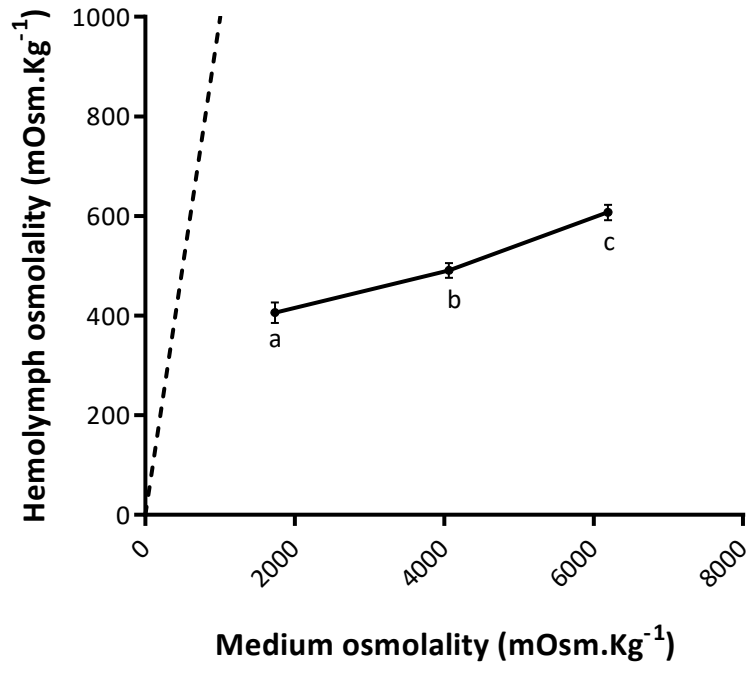
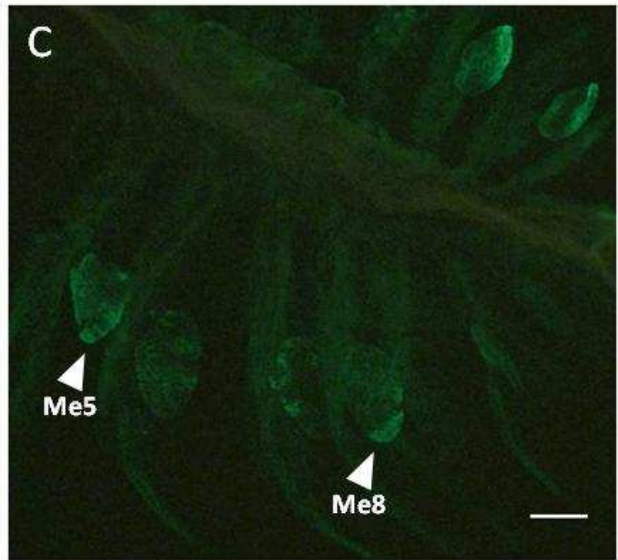
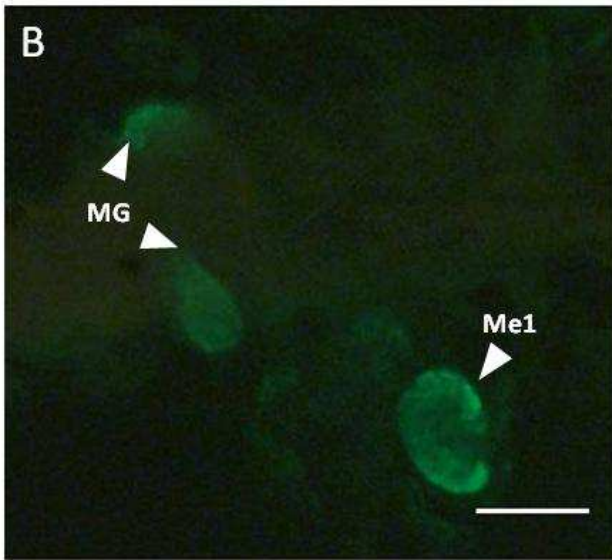
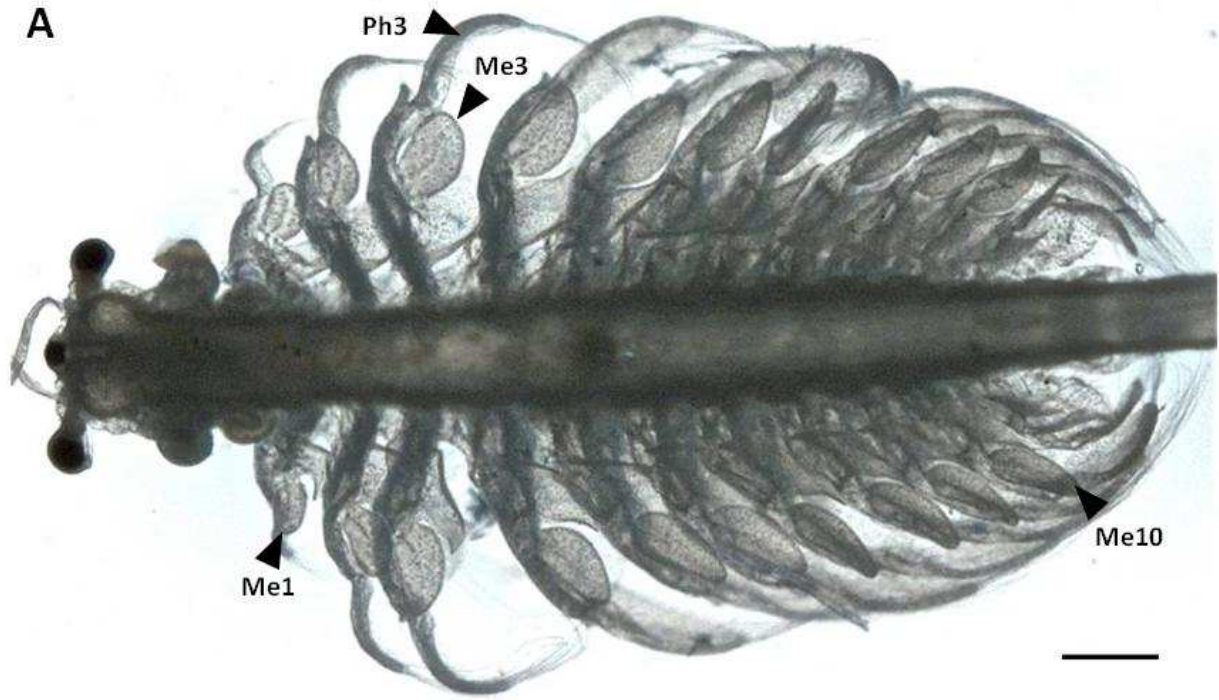


Fig. 2.

657  
658  
659



660  
661

Fig. 3.

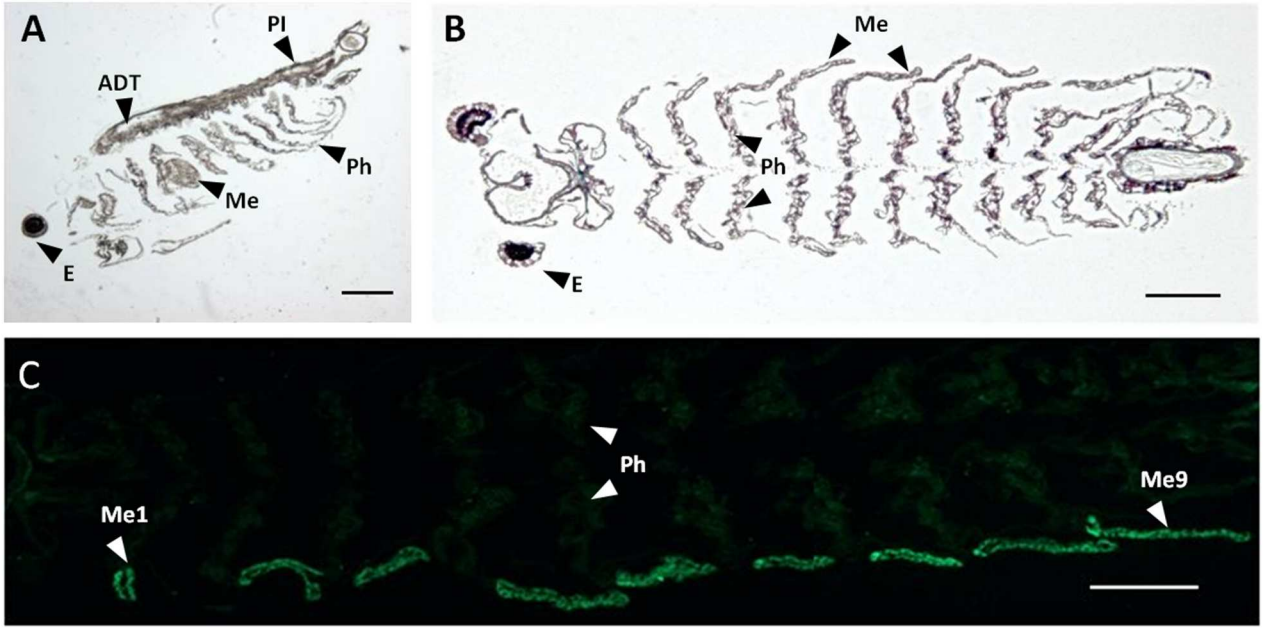


Fig. 4.

662  
663  
664



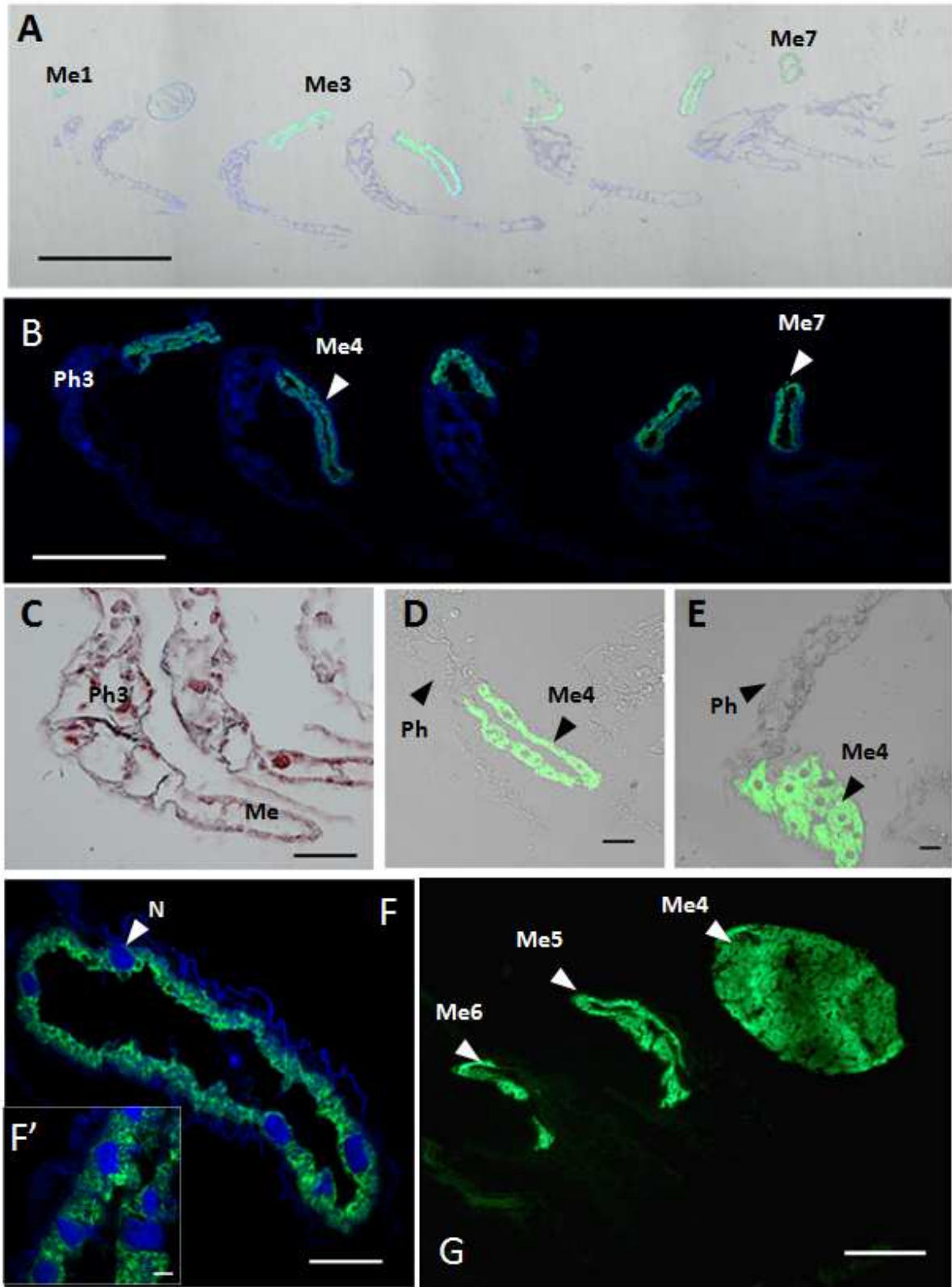


Fig. 5.

665  
666  
667



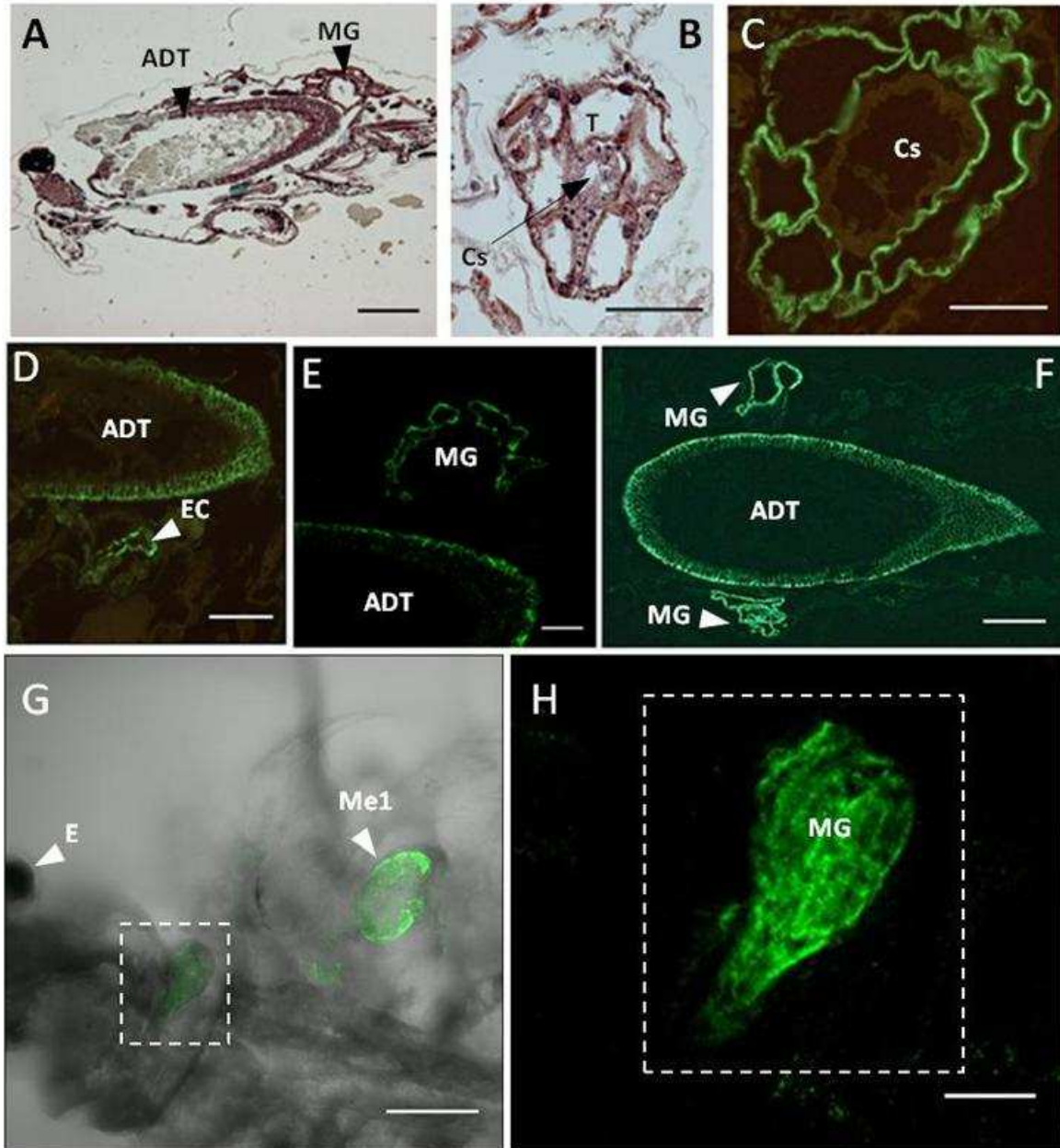


Fig. 6.

668  
 669  
 670  
 671

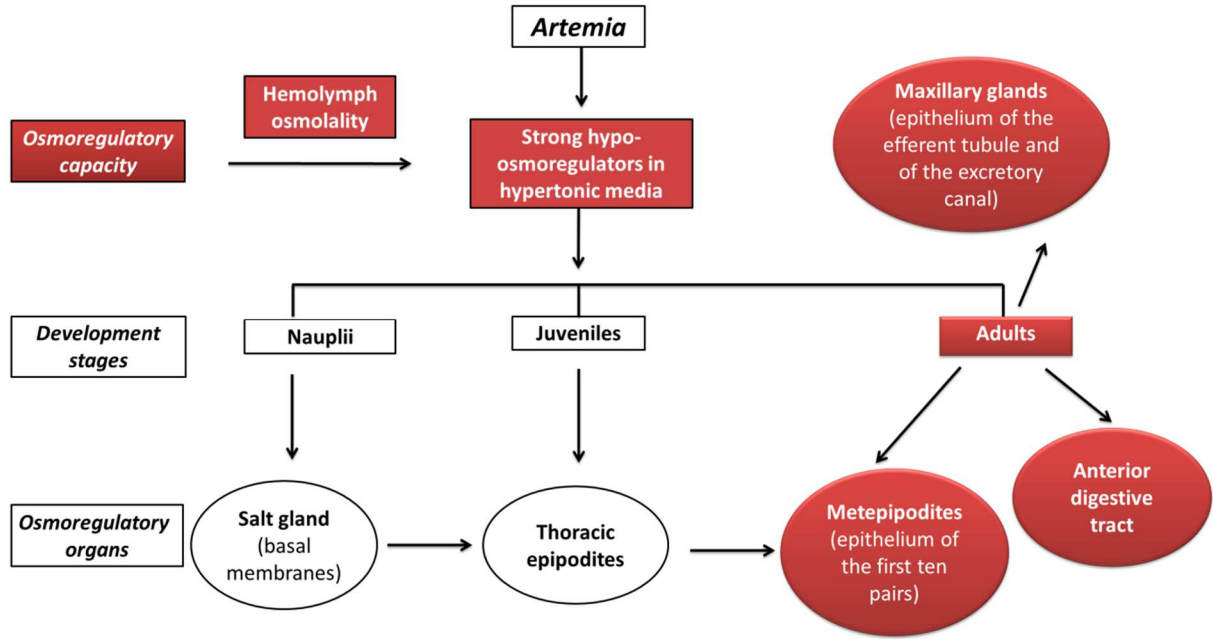
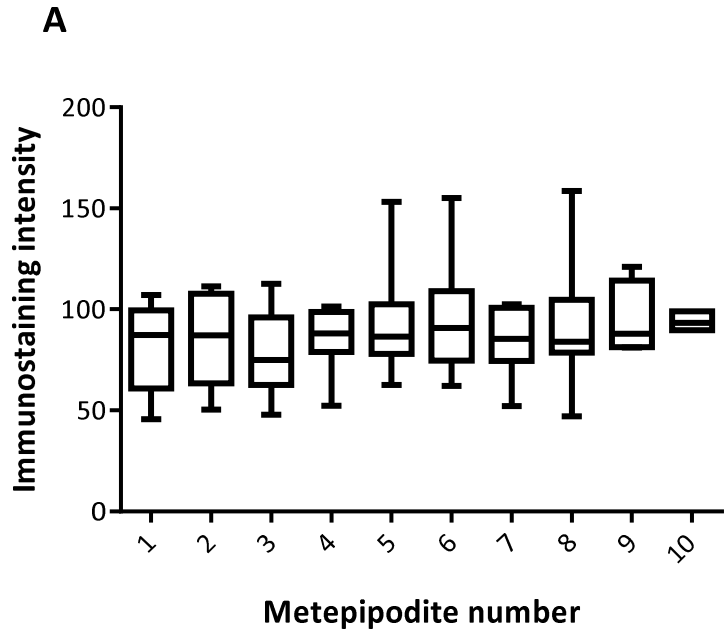


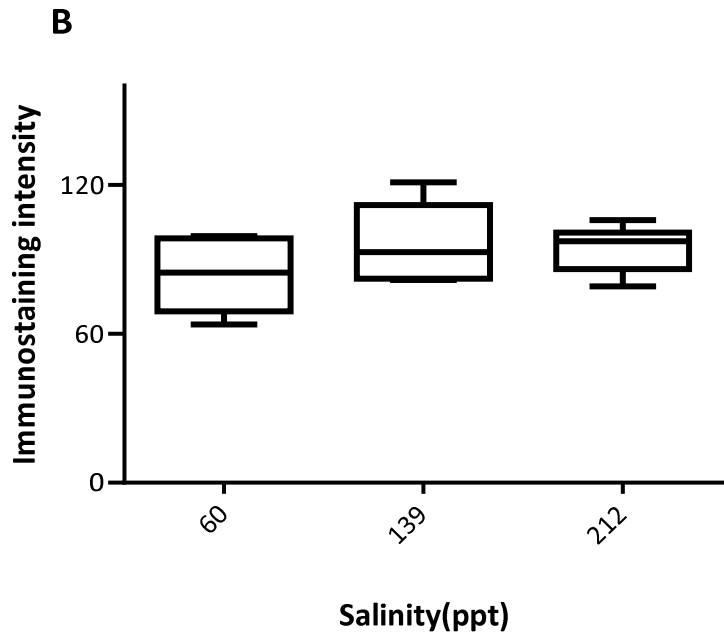
Fig. 1S.

672  
673  
674  
675  
676  
677

678  
679



680  
681



682  
683  
684  
685  
686

Fig. 2S.